

# RESEARCH ON PULSE INFRARED THERMAL WAVE DETECTION TECHNOLOGY FOR HONEYCOMB SANDWICH STRUCTURE DEFECTS

by

*Qing-Ju TANG<sup>a,\*</sup>, Zhuo-Yan GU<sup>a</sup>, Hong-Ru BU<sup>a</sup>, and Rui XIE<sup>a</sup>*

<sup>a</sup> School of Mechanical Engineering, Heilongjiang University of Science and Technology,  
Harbin 150022, China

*Through the method of numerical simulation, the detection rules of different defect characteristics and the detection effect of detection process parameters on different defects were explored. The optimal detection process parameters for GFRP/NOMEX honeycomb sandwich structure specimens with delaminating, debonding, water accumulation and glue plugging defects were obtained. Experimental research was carried out to verify its detection effect for actual tests. The result is that the technology under this parameter can get better defect detection effect.*

**Keywords:** *honeycomb sandwich structure, pulse infrared thermal wave detection, simulation analysis*

## Introduction

Honeycomb sandwich [1-5] structure is widely used in all walks of life, because of its advantages of light weight, high specific strength and low cost. Modern requirements for all aspects of products are getting higher and higher. Its performance testing and fault diagnosis have gradually become the core of comprehensive technical support. In the process of product production to the market, some damage and defects are prone to occur in each process, such as abnormal glue quantity [4] and debonding [5-6] in the process of material production, skin delaminating [7-8] in the process of service, and water accumulation [1-2,5-6] in the honeycomb core after rain and condensate water due to the decrease of sealing performance caused by load. Water accumulation will further lead to degumming, weight gain, icing and damage to the internal honeycomb structure. The internal defect area will expand over time, which will greatly affect the reliability and service life of the machine. Therefore, effective detection methods must be adopted. Under the premise of not causing secondary damage to the measured object, detect whether there is an abnormality in its internal structure, and determine and identify the defects at the abnormal place.

Infrared thermal wave non-destructive testing technology [9-10] has been rapidly developed in recent decades. Compared with conventional non-destructive testing methods, it has the point of fast detection speed, and easy quantitative analysis. This paper will use the technology to detect honeycomb sandwich structure with delaminating, debonding, water accumulation and glue plugging.

---

\* Corresponding author, e-mail: tangqingju@126.com

## Detection principle

### *Infrared thermal wave nondestructive testing theory*

Heat conduction is a behavior that microscopic particles lead to thermal diffusion through random thermal motion, that is, to achieve heat transfer. The relationship between temperature and heat is described by the Fourier's law, given as [10]:

$$q(r,t) = -k\nabla T(r,t) \quad (1)$$

where  $\nabla T(r,t)$  is the temperature gradient,  $k$  is the thermal conductivity of the material, and  $q(r,t)$  is the heat flux.

For anisotropic materials, the well-known 3-D heat conduction differential equation can be expressed as:

$$\frac{\partial}{\partial x} \left( k_x \frac{\partial T}{\partial x} \right) + \frac{\partial}{\partial y} \left( k_y \frac{\partial T}{\partial y} \right) + \frac{\partial}{\partial z} \left( k_z \frac{\partial T}{\partial z} \right) = \frac{\partial T}{\partial t} \quad (2)$$

where  $k_x, k_y$ , and  $k_z$  are the thermal conductivities of the material in the three directions,  $c$  is the specific heat capacity, and  $\rho$  is the density.

### *Pulsed thermal imaging detection principle*

The reflective pulse excitation detection technology is used to detect the defects of GFRP/NOMEX honeycomb sandwich structure specimens with delamination, debonding, water accumulation and glue plugging defects. The principle of the technology is shown in fig. 1 The surface of the specimen is excited by the excitation of the pulse waveform generated by the halogen lamp controlled by the computer. If there are defects in the sample, the abnormal temperature can be observed by the infrared thermal imager.

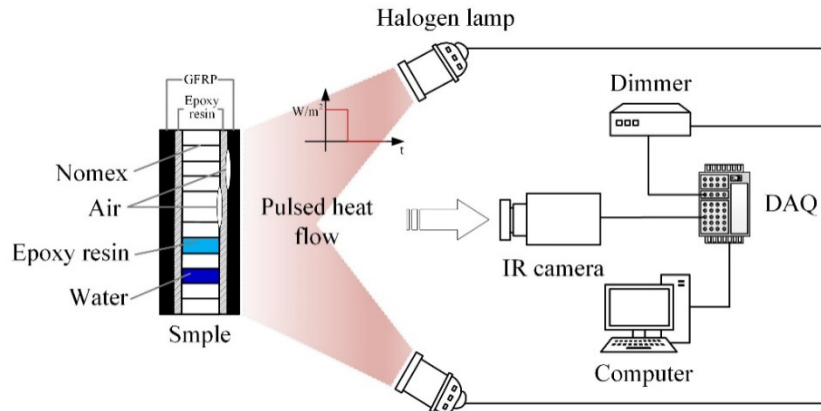


**Figure 1. The schematic diagram of pulse infrared thermal wave detection technology**

Due to the heat transfer capacity of the medium at the defect, the defects are divided into thermal insulation defects and thermal conductivity defects. The surface temperature of the thermal insulation defect specimen will be higher than that of the non-defective part, and the heat map shows obvious “hot spots”. The surface temperature of the thermal conductivity defect specimen is lower than that of the defect-free place, and the heat map shows obvious “cold spot”, as shown in fig.2.

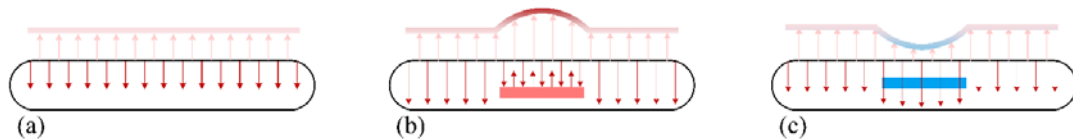


**Figure2. Heat transfer diagram of different defects; (a)without defects, (b) containing thermal insulation defects and (c) containing thermal conductivity defects**

### Numerical simulation analysis

The GFRP/NOMEX honeycomb sandwich structure model was established for simulation analysis. The specimen was bonded by 0.7mm GFRP skin through 0.1 epoxy resin and 4mm honeycomb core. The overall geometric size was 160mm × 140mm × 5.6mm.

When the halogen is used as the excitation source, the light spot formed by the light source in the detection area is approximately Gaussian distribution. When it is used as the excitation source, the heat flux density distribution reads [11]:

$$q(x, y) = \frac{P}{\pi d^2 / 4} \exp\left[-\frac{(x - x_0)^2 + (y - y_0)^2}{d^2 / 4}\right] \quad (3)$$

where  $d$  is the beam waist diameter,  $P$  is the peak power, and  $(x_0, y_0)$  is the coordinate of the beam center position.

Set the pulse width to 7 s. The peak power is set to be 2000 W, and the waist diameter of the light source is 0.6 m. The heat flux density distribution intensity varies according to formula (3). There is a complete contact heat exchange between the laminates. The heat transfer coefficient is  $h = 10.0 \text{ W}/(\text{m}^2 \cdot ^\circ\text{C})$ , the surface emissivity  $\varepsilon = 0.9$ , and the initial temperature is  $20^\circ\text{C}$ . The sampling time is set to 30 s. The surface heat map of the specimen at different times is shown in fig. 3.

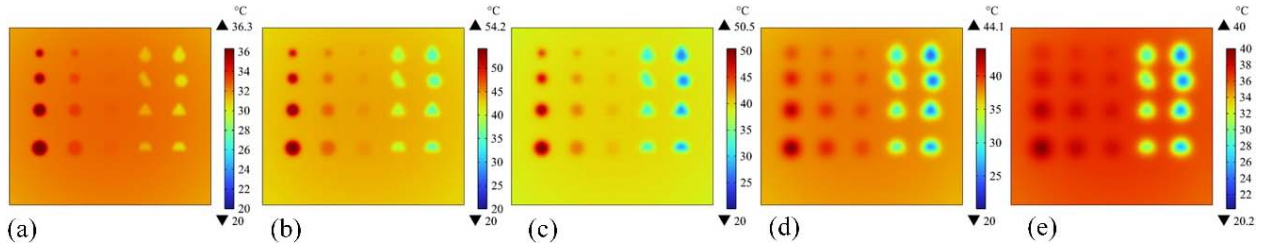


**Figure3. Temperature field distribution on the surface of the specimen at different times; (a)  $t=3\text{s}$ , (b)  $t=7\text{s}$ , (c)  $t=10\text{s}$ , (d)  $t=20\text{s}$  and (e)  $t=30\text{s}$**

When 3seconds. Except for the third column, the defects are clearly visible. When 7seconds, the defects are all displayed, and the edge contour of the defects is clear. At 10 seconds, the specimen has entered the heat dissipation stage. The defects are more obvious but the edges have begun to blur. At 20 seconds, the defect edge cannot be confirmed. At 30 seconds, the specimen is constantly approaching the thermal equilibrium.

The thermal contrast is used as the evaluation index, together with the temperature and temperature difference to quantify the detection ability of the technology for different characteristic defects, and to find the best process parameters for detection. The calculation formula for the thermal contrast is given as follows:

$$C(t) = \left| \frac{[T_D(t) - T_D(0)] - [T_S(t) - T_S(0)]}{T_S(t) - T_S(0)} \right| \quad (4)$$

where  $T_D$  is the temperature of the excitation surface at the defect,  $T_S$  is the temperature of the excitation surface at the defect-free point,  $T_D(0)$  is the initial temperature of the excitation surface at the defect, and  $T_S(0)$  is the initial temperature of the excitation surface at the defect-free point.

*The influence of defect characteristics and geometric parameters on the detection effect*

#### (1) Impact of defect categories

In order to explore the surface temperature signals of different types of defects after excitation. Figure.4 is the average temperature and contrast of each type of defect.

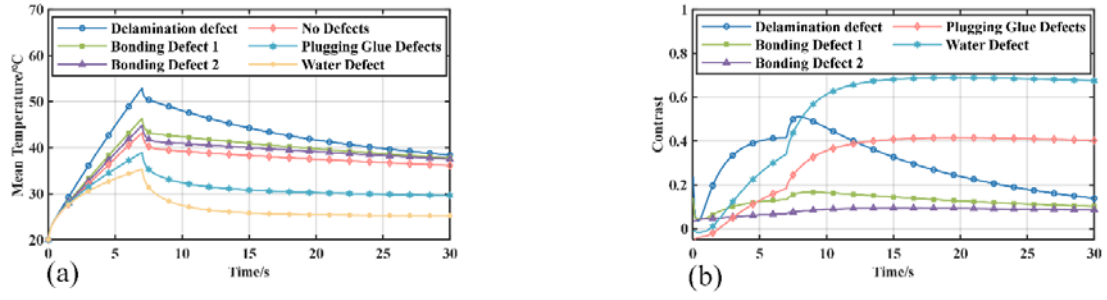


**Figure4. The influence of different types of defects on the surface temperature and contrast of the specimen; (a) Temperature and (b) Contrast**

The average temperature and contrast at the delaminating defects are higher than those at the debonding defects, that is, when the defect area is the same, the delaminating defects are easier to detect than the debonding defects. The temperature of specimens at the water accumulation is lower than that at the glue plugging place, and the contrast at the water accumulation is higher than that at the glue plugging place, that is, in the case of the same amount of water and glue, the water accumulation is easier to detect than the glue plugging.

(1) The influence of the diameter and depth of thermal insulation defects on the detection effect

As shown in fig.5, the temperature and contrast curves of different diameter defects with a buried depth of 0.5 mm and different depth defects with a diameter of 12 are shown.

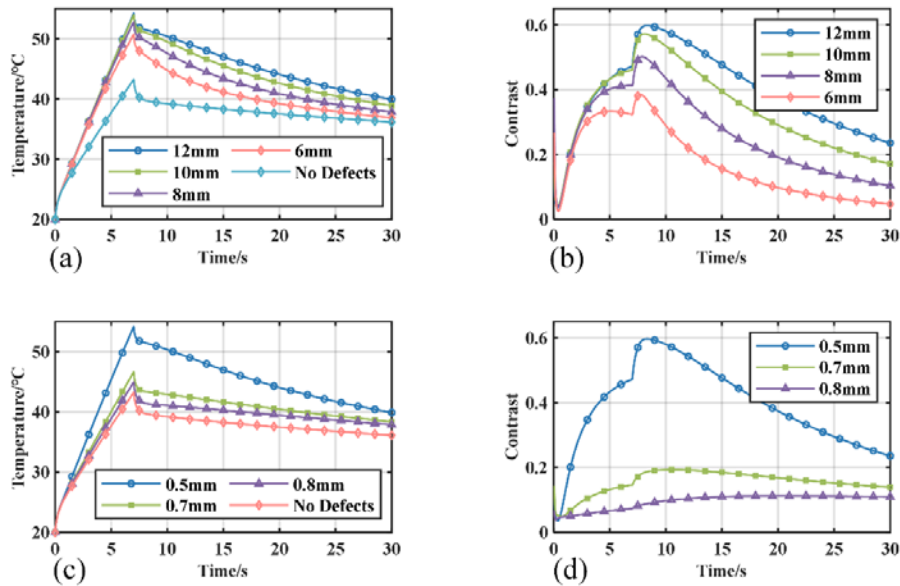


**Figure5. The influence of thermal insulation defect diameter and buried depth on surface temperature and contrast; (a) and (c) are temperature, (b) and (d) are contrast**

The larger the diameter of the thermal insulation defect, the shallower the buried depth, the higher the surface temperature of the corresponding test piece, the higher the contrast, and the easier the defect is detected.

(3) The influence of defect water accumulation

The thermal conductivity defect takes water accumulation as an example. Figure.6 is the surface temperature and contrast of the defect specimens with different water accumulation. The amount of water is 8-5 honeycomb holes.

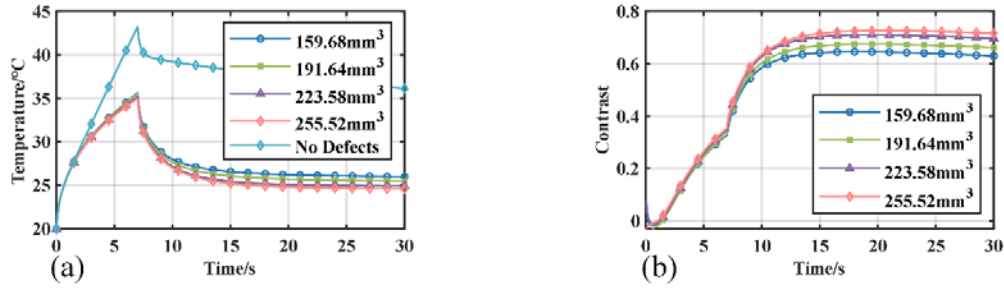


**Figure6. The effect of different water volume on surface temperature and contrast. (a) Temperature and (b) Contrast**

The greater the amount of water added, the greater the temperature differences between the surface of the defect specimen and the defect-free place, and the greater the contrast, indicating that the defect is more easily detected.

*The influence of detection process parameters on the detection effect*

The pulse excitation with different pulse width and light source power on the temperature signal of defect surface is studied, the optimal detection parameters are searched. The layered defect with the largest diameter represents the defect of thermal insulation performance, and the water defect with the largest water accumulation represents the defect of thermal conductivity.

(1) The influence of pulse width

Figure.7 shows the temperature difference and contrast between defects and no defects when the pulse width is 7s, 9s, 11s and 13s under the light source power of 2000W.

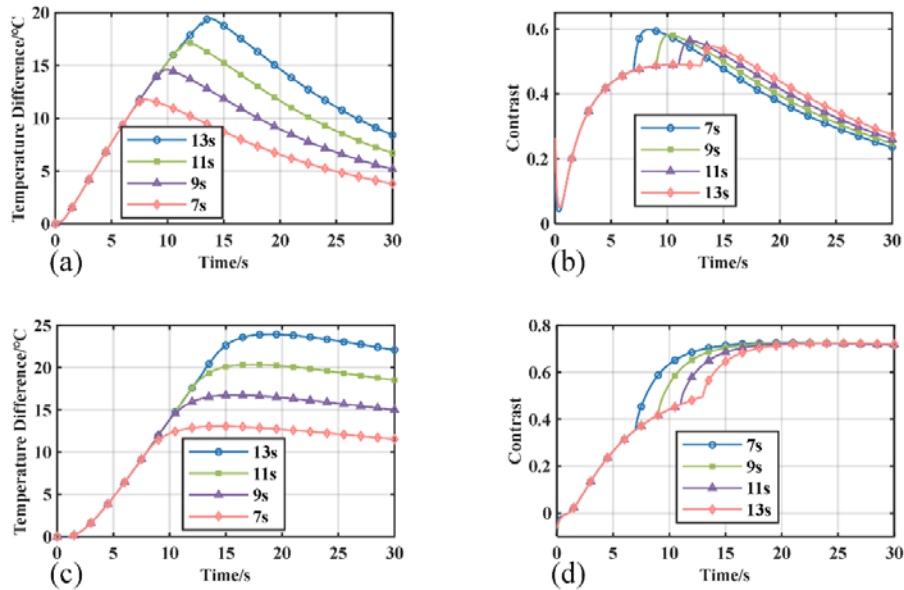


**Figure 7. The influence of pulse width on the detection effect of defects; (a) and (c) are temperature difference, (b) and (d) are contrast**

The larger the pulse width, the greater the final temperature difference during the excitation stage. The smaller the pulse width, the greater the contrast improvement in the early cooling stage, and the easier the defect is detected. Therefore, in the case where a certain temperature difference can be generated, a smaller pulse width is selected. Considering the detection effect, the pulse width of the heat source is finally set to 7s.

(2) Impact of power

Figure.8 is the temperature and contrast of the surface of the thermal insulation defect and the thermal conductivity defect when the pulse width is 7s and the light source power is 1400W, 1600W, 1800W and 2000W, respectively.

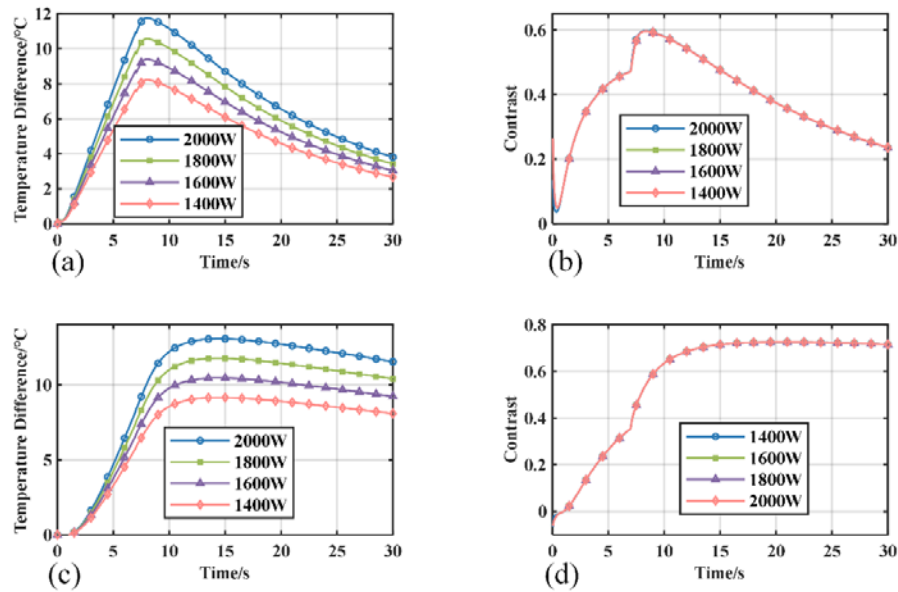


**Figure8. The influence of light source power on the detection effect of defects; (a) and (c) are temperature difference, (b) and (d) are contrast**

The temperature difference increases with the increase of the power of the light source. Different light source powers have no significant effect on the contrast of defects. Therefore, under the premise of ensuring that the specimen will not be destroyed again due to high temperature, 2000 W with the largest temperature difference can be selected as the test heat source power. Figure. 3 shows that the peak surface temperature of the specimen is 54.2 °C, which is within the acceptable range of the specimen.

### Experiment and analysis of its results

As shown in fig.9, for the test system diagram, the power of the halogen lamp light source is set to 2000 W, and the pulse width of the pulse excitation is 7 s. Figure. 10 is the specimen.

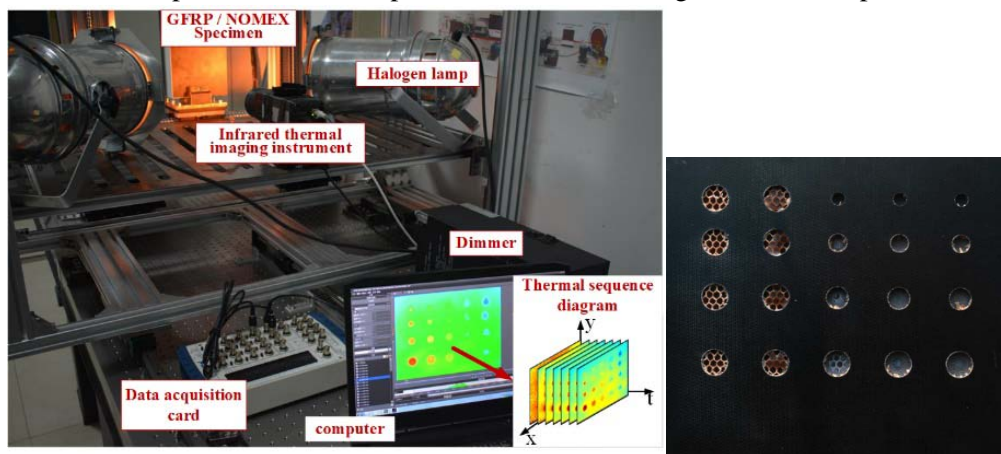


**Figure9. Experimental System Figure10. Specimen**

Figure. 11 (a) is the heat map at the peak time of the temperature. The prefabricated defects in the specimen have been displayed. The defect display effect is good and the contour is clear, but there are problems of noise and uneven heat. Figure.11 (b) shows the result of subtracting the first

frame. It can be observed that the noise in the heat map is reduced, and the defects in the fourth line are more obvious around it.

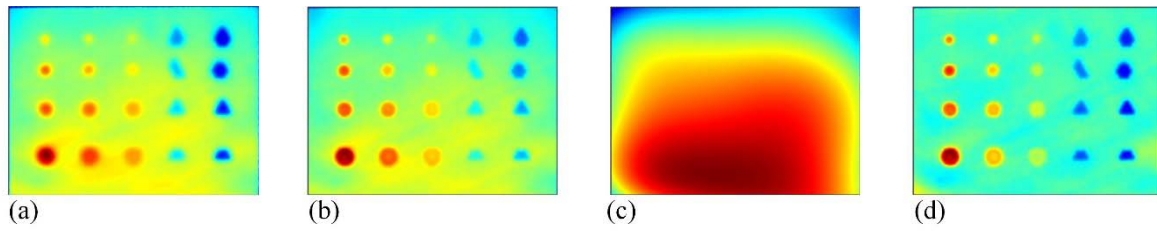


**Figure11. Image processing; (a) A frame heat map, (b) The heat map after subtracting the first frame, (c) Fitting background and (d) Heat map after subtracting the fitting background**

To improve the detection effect of defects, a least squares fitting was performed on the heat map after subtracting the first frame to form a surface that basically matches the temperature distribution field. The results are shown in fig. 11(c), which was subtracted from the heat map in fig. 11(b) to obtain the results shown in fig. 11(d). This solves the problem of thermal unevenness and further improves the defect detection effect. The detection effect of water accumulation and glue blockage defects is particularly significant, and the defect display is clearer, strong contrast with the background and clear contour of all defect edges are conducive to quantitative research of defects.

## Conclusion

The detection process of GFRP/NOMEX honeycomb sandwich structure with prefabricated defects was numerically simulated. The simulation results indicate that pulse infrared thermal wave detection technology can effectively detect delamination, debonding, water accumulation, and adhesive blocking defects. Among insulation defects with the same diameter, delamination defects are more easily detected than debonding defects. Among thermal conductivity defects with the same foreign material content, water accumulation is easier to detect than adhesive blockage defects. Moreover, the larger the diameter of thermal insulation defects and the shallower their burial depth, the easier they are to be detected. The larger the amount of water accumulation and adhesive blockage in thermal conductivity defects, the easier they are to be detected. At the same time, according to the optimal process parameters obtained by simulation, the pulse width is 7 s and the power is 2000 W for experimental research. The results showed that the use of subtracting the first frame and subtracting the fitting background operation alleviated the noise interference and thermal unevenness issues in the experiment, further improving the defect detection effect and laying the foundation for quantitative defect detection.

## Acknowledgments

This project is supported by Natural Science Foundation of Heilongjiang Province (Grant No. JQ2023E011).

## Nomenclature

$r$  -spatial variable, [m]  $x, y, z$  - heat transfer direction, [-]  
 $t$  -time variable, [s]  $\nabla T(r, t)$  - temperature gradient, [K/m]  
 $q(r, t)$  - heat flux, [W/m<sup>2</sup>]  $k_x, k_y, k_z$  - thermal conductivity, [W/(m·°C)]

## References

- [1] Tian, Y. P., *et al.*, Detecting Water in Honeycomb Structure by Using Pulsed Phase Thermography (in Chinese), *Infrared Technology*, 28 (2006), 10, pp. 615-619
- [2] Guo, X. W., *et al.*, Study on Pulsed Thermography for Water Ingress Detection in Composite Honeycomb Panels (in Chinese), *Acta Aeronautica et Astronautica Sinica*, 33 (2012), 6, pp.1134-1146
- [3] Yang, F., Research on Infrared Thermal Wave Detection and Convolutional Neural Network Recognition of HSCs Defects (in Chinese), Master. thesis, Harbin Institute of Technology, Harbin, CHN, 2021
- [4] Meola C, *et al.*, Non-destructive Evaluation of Aerospace Materials with Lock-in Thermography. *Engineering failure analysis*, 13(2006), 3, pp. 380-388
- [5] Fang, W. M., Research on The Technology of GFRP/NOMEX Honeycomb Sandwich Structure Defects Detection Using Infrared Thermal Wave Testing Method (in Chinese), Master. thesis, Heilongjiang University of Science and Technology, Harbin, CHN, 2022
- [6] Tang, Q. J., *et al.*, Defect Detection of GFRP/Nomex Honeycomb Sandwich Structure by Linear Frequency Modulation Infrared Thermal Imaging. *Thermal Science*, 25(2021), 6 Part B, pp. 4611-4619
- [7] Tang, Q. J., *et al.*, Defect Detection of GFRP Laminates by Barker Code Modulation Excitation Infrared Thermal Imaging. *Thermal Science*, 27(2023), 1 Part B, pp. 447-454
- [8] Tashan, J, Al-Mahaidi R., Investigation of The Parameters That Influence the Accuracy of Bond Defect Detection in CFRP Bonded Specimens Using IR Thermography. *Composite Structures*, 94(2012), 2, pp. 519-531
- [9] Bu, C. W., *et al.*, Infrared Thermal Imaging Detection of Debonding Defects in Carbon Fiber Reinforced Polymer Based on Pulsed Thermal Wave Excitation, *Thermal Science*, 24(2020), 6 Part B, pp. 3887-3892
- [10] Tang, Q. J., Research on The Key Technology of SIC Coating Defects Detection Using Pulsed Infrared Thermal Wave Non-destructive Testing Method (in Chinese), Ph. D. thesis, Harbin Institute of Technology, Harbin, CHN, 2014
- [11] An, S. J., Research on Pulsed Infrared Thermal Wave Detection Technology for CFRP Laminate Defects (in Chinese), Master. thesis, Heilongjiang University of Science and Technology, Harbin, CHN, 2023

Paper submitted: June 22, 2023

Paper revised: August 21, 2023

Paper accepted: November 22, 2023